J Mater Sci (2007) 42:8489–8495
DOI 10.1007/s10853-007-1752-1

Thermodynamic analysis of thermite reactions for synthesizing Ni-based alloys

Wenjun Xi · Heping Zhou · Chaoli Ma · Huiping Duan · Tao Zhang

Received: 26 August 2006 / Accepted: 9 April 2007 / Published online: 23 June 2007

Abstract The equilibrium compositions of a thermite reaction system (Fe_2O_3+Cr_2O_3+CrO_3+NiO+O_2+N_2+TiO_2+C+S+CaO+Al), which was used to prepare Ni-based alloys, were predicted by means of the free energy minimization method. The effects of the reactant contents on the equilibrium compositions and the adiabatic temperature of the thermite reaction system were analyzed. The microstructure of the Ni-based alloys was investigated. The thermodynamic analysis indicated that the products of the thermite reaction system contained primarily Al_2O_3, Fe, Ni, Cr, Ni_3Al and NiAl, due to impurities C, N_2 and S in the raw materials, there could also exist TiC, Cr_7C_3, CrN, CaS and TiN in the equilibrium products. The amount of Ni_3Al and NiAl in the products increased with increase of the aluminum content in the starting materials. The microstructure investigation showed that the Ni-based alloys consisted of austenite, ferrite, Ni_3Al and NiAl. The existence of Ni_3Al and NiAl in the Ni-based alloys reconciled with the predictions of thermodynamic analysis, suggesting the free energy minimization method is useful in designing advanced materials with multiple components by thermite reaction technique.

W. Xi (✉) · C. Ma · H. Duan · T. Zhang
School of Materials Science and Engineering, Beijing University of Aeronautics and Astronautics, Beijing 100083, P.R. China
e-mail: xiwj@buaa.edu.cn

H. Zhou
Department of Materials Science and Engineering, Tsinghua University, Beijing 100083, P.R. China

Introduction

The thermite reaction describes a broader class of reactions involving a metal reacting with a metallic or a non-metallic oxide to form a more stable oxide and the corresponding metal or non-metal of the reactant oxide. This type of reaction is characterized by a large heat release which is often sufficient to heat the product phases above their melting points. In recent years, the thermite reaction has been used to expand applications in materials synthesis [1, 2]. For example, the centrifugal-thermite process developed from the thermite reaction and centrifugal casting has been used to fabricate ceramic-lined composite steel pipes that have been applied in industry [3–5].

Recently, we have used the centrifugal-thermite reaction process to prepare a Ni-based alloy lined composite steel pipe [6–8]. The thermite reactions employed to produce the Ni-based alloy are generally expressed as follows

$$Fe_2O_3 + 2Al = 2Fe + Al_2O_3, \quad \Delta H_{298} = -836\,kJ \qquad (1)$$

$$Cr_2O_3 + 2Al = 2Cr + Al_2O_3, \quad \Delta H_{298} = -530\,kJ \qquad (2)$$

$$CrO_3 + 2Al = Cr + Al_2O_3, \quad \Delta H_{298} = -1094\,kJ \qquad (3)$$

$$3NiO + 2Al = 3Ni + Al_2O_3, \quad \Delta H_{298} = -928\,kJ \qquad (4)$$

According to these chemical equations (Eqs. 1–4), the reaction products are merely composed of pure metals (Fe, Ni, and Cr) and Al_2O_3. However, a large proportion of intermetallic compounds were detected in the products together with Fe, Ni, Cr and Al_2O_3 [7]. Clearly, the chemical equations listed above cannot describe the phase equilibria and phase compositions exactly. Moreover, the raw materials contain some impurities, such as O_2, N_2, TiO_2, S and C, which participate in the thermite reactions

and, consequently, affect the phase equilibria in the resultant alloys. The information about the product compositions is helpful not only to predict the quantities of products, but also to design the composition and morphology of the prepared materials. Therefore, it is necessary to perform a thermodynamic analysis using an effective method to predict the product compositions of the thermite reactions.

In the present study, a thermodynamic method, namely, the free energy minimization method [9, 10], was employed to analyze the thermite reactions process, which was used to prepare the Ni-based alloys. To validate the results obtained by the thermodynamic analysis, the microstructure of the thermite-reacted Ni-based alloys was investigated by various techniques, such as scanning electron microscopy (SEM), transmission electron microscopy (TEM) and X-ray diffraction analysis (XRD).

Preparation of the Ni-based alloys and thermodynamic analysis

Preparation of the Ni-based alloys

Figure 1 schematically shows the centrifugal-thermite process used in this study. The Al, NiO, Cr_2O_3, CrO_3, Fe_2O_3 and CaO powders were blended and used as starting materials. A low carbon steel pipe with an outer diameter of 76 mm and wall thickness of 5 mm and a length of 100 mm was mounted on a centrifugal machine. The steel pipe was loaded with the starting materials, which was immediately ignited by a tungsten filament once a given rotation velocity of the centrifugal machine was reached. During the reactions, the oxides were reduced by aluminum (Al), resulting in formation of metal Fe, Ni, Cr and alumina (Al_2O_3). The Combustion temperature (i.e. adiabatic temperature) was sufficiently high that all reacted products became liquid. Due to the centrifugal force field, the molten Fe, Ni and Cr (with a density higher than that of alumina) flowed to the inner surface of the steel pipe. The alumina (with lower density than the molten alloy) covered the alloy and formed a slag layer. The constituent phases in the alloy layer were analyzed using XRD. The morphology and structure of the alloy layer were investigated using SEM and TEM.

Thermodynamic analysis

The thermite reactions generated a large amount of heat which was sufficient to melt all the products rapidly, so that an approximate equilibrium state was obtained within a relatively short time. Therefore, the product compositions were calculated using equilibrium thermodynamic analysis [10].

The total free energy, G, of the thermite reaction system can be expressed as:

$$G = \sum_i n_i \mu_i \tag{5}$$

where n_i denotes the number of mole of substance i, and μ_i is the chemical potential defined as

$$\mu_i = \mu_i^0 + RT \ln a_i \tag{6}$$

where a_i is the activity, μ_i^0 is the standard chemical potential.

All the condensed substances in the thermite system were considered to be pure with unit activities. Therefore, Eq. 6 can be written as:

$$\mu_i = \mu_i^0 = g_i^0 \tag{7}$$

where g_i^0 is the standard free energy change of species i.

For the gaseous species, such as N_2, O_2, which are treated as ideal gases, the activities a_i are equal to the partial pressures p_i

$$a_i = p_i = (n_i/N)P \tag{8}$$

N is the total number of moles and P is the total pressure in gas phase. From Eqs. 5–8, it follows that

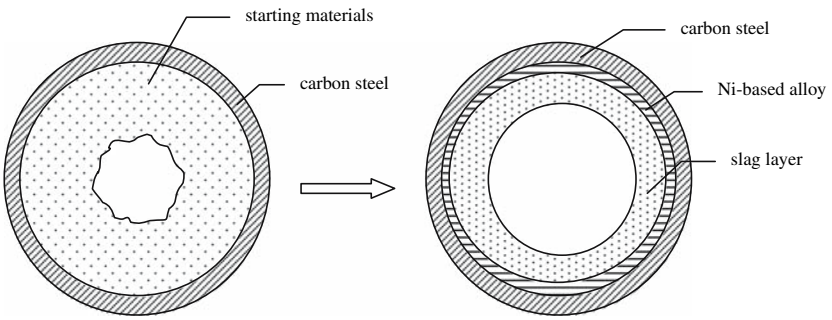

Fig. 1 Schematic representation of the centrifugal-thermite process

$$G = \sum_{i=1}^{l} n_i^g [g_i^g + RT \ln P + RT \ln(n_i^g / N)] + \sum_{i=1}^{s} n_i^c \cdot g_i^c \quad (9)$$

where g and c represent the gaseous species and the condensed species, respectively. l is the number of gaseous species; s is the number of condensed substances. The value of g_i can be determined from entropy and enthalpy data by

$$g_i = \Delta H_i - T\Delta S_i \quad (10)$$

ΔH_i and ΔS_i denote the enthalpy change and entropy change of the ith substance, respectively.

Assuming the thermite reaction system to be closed, there is one equation for each element, and the mass balance relations can be written as

$$\sum_{i=1}^{l} d_{ij}^g n_i^g + \sum_{i=1}^{s} d_{ij}^c n_i^c = b_j \quad (j = 1, 2, \ldots, M) \quad (11)$$

where d_{ij} represents the number of atoms of the jth element in a molecule of the ith substance, b_j is the total number of moles of the jth element, and M is the total number of elements.

According to the free energy minimization method, under subsidiary conditions satisfying the mass balance relationships Eq. 11, a set of values of n_i minimized Eq. 9 can be calculated. A Fortran computer program was developed to solve these problems. The thermodynamic data were mainly obtained from Refs. [11–13].

Assuming that there is no heat loss to surroundings, i.e. adiabatic conditions, the total heat, Q, of the thermite system can be calculated from the following equation:

$$Q = -\sum_i \int_{298}^{T} n_i^0 \cdot Cp_i dT + \sum_i \Delta H_i \cdot \Delta n_i \quad (12)$$

where T is the preheating temperature before inducing the thermite reaction; Cp_i is the heat capacity of species i in the solid state; n_i^0 is the number of mole of reactant in the starting materials; Δn_i is the difference of the initial and equilibrium mole numbers of the species i.

The adiabatic temperature T_{ad} can be obtained by solving the following equation

Table 1 Possible phases produced in the thermite reaction system

reactants:
gaseous: O_2 N_2
oxides: Cr_2O_3 CrO_3 TiO_2 CaO NiO Fe_2O_3
metals: Al, Ti
non-metals: C, S
possible products:
metals: Fe Cr Ni
oxides: Al_2O_3
carbides: TiC Cr_3C_2 $Cr_{23}C_6$ Cr_7C_3 Fe_3C
nitrides: AlN CrN Cr_2N TiN Fe_4N
sulphides: FeS Fe_7S_8 CaS
intermetallic compounds: NiAl Ni_3Al $NiAl_3$ Ni_2Al_3 TiAl $TiAl_3$
spinels: $FeAl_2O_4$ $FeCr_2O_4$

$$\sum_i \int_T^{T_m} n_i Cp_i dT + \sum_i n_i H_{im} + \sum_i \int_{T_m}^{Tad} n_i Cp_{li} dT = Q \quad (13)$$

where Cp_{li} is the heat capacity of species i in liquid state. H_{im} is the heat of melting of species i.

From the compositions of the starting materials and the possible products of the thermite reactions, 37 substances were chosen in the thermite system, and are presented in Table 1. It should be noted that the substances or phases chosen in the system may not be very comprehensive; however, the number of elements and substances can be increased if some substances are introduced into the thermite reaction system.

Results and discussion

Results of thermodynamic calculation

Thermodynamic equilibrium products

The compositions of starting materials are listed in Table 2. The impurities of N_2, O_2, TiO_2, C and S were also listed here, where the contents of gaseous species, N_2 and O_2, are estimated by assuming that the porosity of the starting materials is about 30% and all pores are full of air,

Table 2 Composition of the starting materials

Species number	1	2	3	4	5	6	7	8	9	10	11
Molecular formula	O_2	N_2	Cr_2O_3	CrO_3	TiO_2	CaO	Al	NiO	Fe_2O_3	C	S
Compositions (wt%)	0.028	0.109	15.200	2.810	0.098	0.927	28.600	29.700	22.300	0.191	0.090

Table 3 An example of output of an equilibrium composition

Species number and Molecular formula	Contents (wt%)
1. (O_2)	0.0000
2. (N_2)	0.0000
3. (Cr_2O_3)	0.0000
4. (CrO_3)	0.0000
5. (TiO_2)	0.0000
6. (CaO)	0.7698
7. (Al)	0.0000
8. (NiO)	0.0000
9. (Fe_2O_3)	0.0000
10. (C)	0.0000
11. (S)	0.0000
12. (Al_2O_3)	40.9383
13. (Fe)	15.5757
14. (Ni)	0.0000
15. (Cr)	9.9287
16. ($FeCr_2O_4$)	0.0000
17. (Cr_2N)	0.0000
18. (TiC)	0.0000
19. ($Cr_{23}C_6$)	0.0000
20. (Cr_7C_3)	2.1227
21. (Cr_3C_2)	0.0000
22. (CrN)	0.0000
23. (Fe_4N)	0.0000
24. (AlNi)	15.3696
25. ($AlNi_3$)	14.7462
26. (Al_3Ni)	0.0000
27. (Al_3Ni_2)	0.0000
28. ($TiAl_3$)	0.0000
29. (TiAl)	0.0000
30. ($FeAl_2O_4$)	0.0000
31. (CaS)	0.2023
32. (FeS)	0.0000
33. (Fe_7S_8)	0.0000
34. (AlN)	0.2705
35. (TiN)	0.0762
36. (Fe_3C)	0.0000
37. (Ti)	0.0000
Q = –1.3119e + 006 (J)	
T_{ad} = 3.2815e + 003 (K)	

i.e. N_2 and O_2. The CaO is an addition that can improve the fluidity of the molten products by decreasing the melting point of the slag, which is helpful for reducing the inclusions in the alloy [6]. An example of the equilibrium composition predicted by the thermodynamic analysis calculation at 1 atm. and room temperature is presented in Table 3. It can be seen that Ni_3Al, NiAl, CaS, AlN, Cr_7C_3 and TiN were predicted in the products, as well as Al_2O_3, Fe, Ni and Cr described by the chemical Eqs. 1–4. If C and Ti or TiO_2 exist in the starting materials, the carbide TiC could be formed. According to the reaction products predicted, the possible chemical reactions could be speculated, as listed in Table 4. In addition, the occurrence of CaS in the reaction products indicated that CaO can act as desulphurizer.

Table 4 The possible reactions in the thermite reaction system

Products	Possible chemicalreactions
Al_2O_3	$Fe_2O_3 + 2Al = 2Fe + Al_2O_3$
Fe	$Fe_2O_3 + 2Al = 2Fe + Al_2O_3$
Cr	$Cr_2O_3 + 2Al = 2Cr + Al_2O_3$
	$CrO_3 + 2Al = Cr + Al_2O_3$
Ni	$3NiO+2Al = 3Ni + Al_2O_3$
TiC	$3TiO_2 + 4Al + 3C = 3TiC + 2Al_2O_3$
	$Ti + C = TiC$
Cr_7C_3	$7Cr_2O_3 + 14Al + 6C = 2Cr_7C_3 + 7Al_2O_3$
	$7CrO_3 + 14Al + 3C = Cr_7C_3 + 7Al_2O_3$
CrN	$Cr_2O_3 + 2Al + N_2 = 2CrN + Al_2O_3$
	$2CrO_3 + 4Al + N_2 = 2CrN + 2Al_2O_3$
NiAl	$3NiO + 4Al = Ni + 2NiAl + Al_2O_3$
Ni_3Al	$6NiO + 5Al = 3Ni + Ni_3Al + 2Al_2O_3$
$FeAl_2O_4$	$2Fe_2O_3 + 2Al + 2Al_2O_3 = Fe+3FeAl_2O_4$
CaS	$2CaO + 3[S] = 2CaS + SO_2$
TiN	$6TiO_2 + 8Al + 3N_2 = 6TiN + 4Al_2O_3$
	$2Ti + N_2 = 2TiN$
AlN	$2Al + N_2 = 2AlN$

Effect of Al content on the phase compositions of Ni, Ni_3Al and NiAl

The thermodynamic calculation revealed that the aluminum content in the starting materials had pronounced effects on the phase equilibria and phase compositions of the nickel-containing products. Figure 2 shows the changes of Ni, Ni_3Al and NiAl contents as a function of aluminum content. During the calculation process the aluminum content changes and the other reactant contents (in weight) are kept constant. When the aluminum content is below 23 wt% in the starting materials, only nickel exists in the nickel-containing products. When the aluminum content exceeds 23 wt%, the intermetallic compound Ni_3Al starts to be formed in the products. When the aluminum content is in the range of 23–26 wt%, there are two phases, i.e. Ni and Ni_3Al in the nickel-containing products. As the aluminum content increases, the Ni_3Al content increases and the Ni

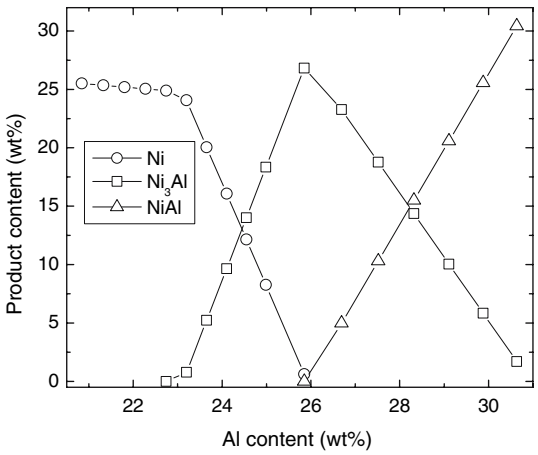

Fig. 2 Effect of aluminum content on the composition of nickel-containing products

content decreases. When the aluminum content reaches about 26 wt%, the Ni_3Al content attains a maximum value of about 25 wt%, while the nickel content tends to zero. At the same time, another intermetallic compound NiAl appears, and its content increases with further increase in aluminum content. The Ni_3Al disappears when the aluminum content reaches about 31 wt%. From the thermodynamic analysis it can be deduced that there is a tendency to attain nickel–aluminum intermetallic compounds in the thermite reaction products under the high aluminum content in the starting materials.

Effects of Al, CrO_3 and CaO contents on the adiabatic temperature

Figure 3 is the thermodynamic calculation results showing the changes of the heat of reaction (Q) and the adiabatic temperature (T_{ad}) of the thermite reaction system as a function of aluminum content. It can been seen that the

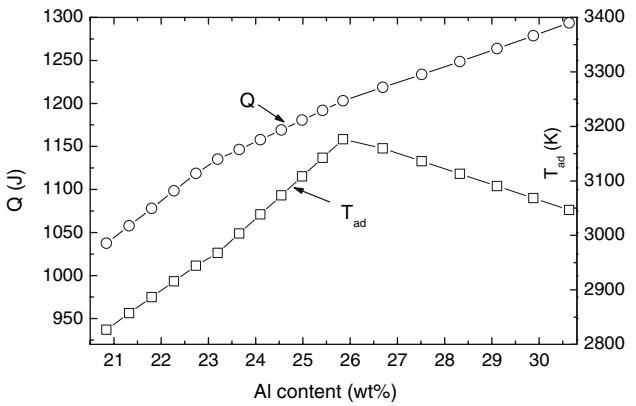

Fig. 3 Effect of aluminum content on the heat of reaction and the adiabatic temperature

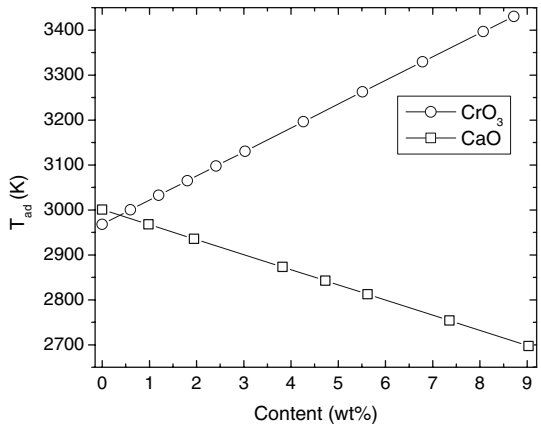

Fig. 4 Effect of CrO_3 and CaO contents on the adiabatic temperature

heat of reaction increases monotonously with the aluminum content, but the adiabatic temperature increases first and then decreases with increase of the aluminum content and it reaches the maximum value at about 26 wt% Al. These phenomena may be related to the fact that the adiabatic temperature not only depends on the heat of reaction, but also relates to the kinds, number, heat capacity and heat of melting of the products. On increasing the aluminum content, Ni_3Al, NiAl are formed in the products besides Al_2O_3, Fe, Cr and Ni. Because of the rise in the number of products, more the heat of reaction may be absorbed when they are heated and melted. If the absorbed heat is more than that generated, the adiabatic temperature of reaction system will be lowered.

Figure 4 presents the thermodynamic calculation results showing the changes of the adiabatic temperature (T_{ad}) of the thermite reaction system as a function of CrO_3 and CaO contents in the starting materials. From the thermodynamic calculation, a certain amount of Cr_2O_3 in the starting materials is replaced by CrO_3. The adiabatic temperature increases linearly with the content of CrO_3, and an increase in the amount of CrO_3 to 8 wt% produces an increase in the adiabatic temperature of about 400 K, which is related to the large heat of reaction (Al+CrO_3), as given in Eq. 3. On the contrary, addition of CaO to the starting materials reduce the adiabatic temperature because some CaO remain after which react with the sulphur and absorb some of the heat of reaction.

Microstructural observations of the synthesized Ni-based alloys

Figure 5 shows the SEM back-scattered electron images of the Ni-based alloy layer. Figure 5a is a cross-section of the Ni-based alloy layer, with the surface adjacent to the steel tube on the right and the surface adjacent to the slag layer on the left. The structure near the surface in contact with

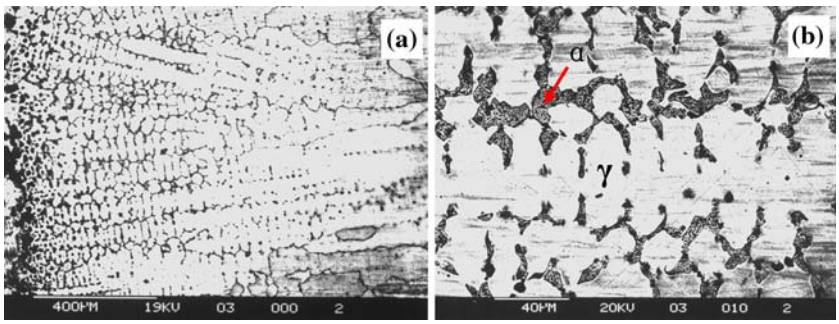

Fig. 5 SEM back-scattered electron image of the Ni-based alloy layer. (**a**) cross-section of the Ni-based alloy layer, the left is the surface adjacent to the slag layer; the right is the surface adjacent to the steel tube, (**b**) the dendritic-grained region

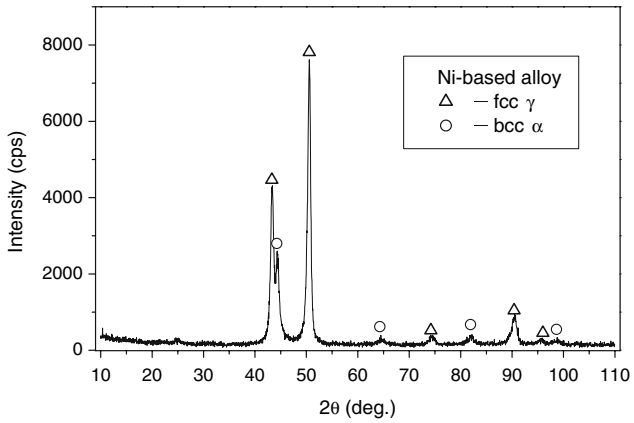

Fig. 6 X-ray diffraction data from the centrifugal-thermite process synthesized Ni-based alloy

the low carbon steel surface grew rapidly in the direction of heat flow, i.e. perpendicular to the wall of the carbon steel. This led to the formation of columnar grains. Near the surface in contact with the slag layer at high temperature, there was evidence of microsegregation, resulting in the formation of a cored dendritic structure (Fig. 5b). The structure appears finer in this area than near the steel substrate surface.

The Ni-based alloy consisted primarily of fcc austenite (γ phase) and bcc ferrite (α phase), as identified by XRD and shown in Fig. 6. Transmission electron microscopy microstructural analysis revealed that the columnar and dendritic grains were the austenite phase, with a thin ferrite layer at the austenite grain boundaries. A large number of fine precipitates were observed in the austenite region, as shown in Fig. 7. Those precipitates were identified as the Ni_3Al phase (γ') with an $L1_2$ structure (Cu_3Au prototype) and a grain size of about 20 nm. The lattice parameters of Ni_3Al and γ are nearly equal, suggesting the possibility that the Ni_3Al is coherent with the matrix γ, similar to Ni_3Al in conventional nickel-based superalloys [14]. Another intermetallic compound NiAl (β) with a B2 structure (CsCl prototype) precipitated in the ferrite as shown in Fig. 8. The orientation relationship between the NiAl and the ferrite has been determined to be $(110)_\beta$ // $(110)_\alpha$, $[001]_\beta$ // $[001]_\alpha$. The B2-ordered structure is a derivative of the bcc structure, and the lattice parameter of stoichiometric NiAl (0.2880 nm) is close to that of α ferrite (0.2876 nm), therefore, NiAl should be coherent or semicoherent with the α matrix. A similar relationship of NiAl with Cr phase has been reported for the NiAl-Cr composite [15]. The Ni_3Al and NiAl formed in the austenite and ferrite phases, respectively, and this may be ascribed to the low interface energy resulting from the coherent phase boundary.

From the XRD pattern of the Ni-based alloy (Fig. 6), the Ni_3Al and NiAl can not be observed because their diffraction peaks almost fully coincide with those of austenite and ferrite, respectively [16].

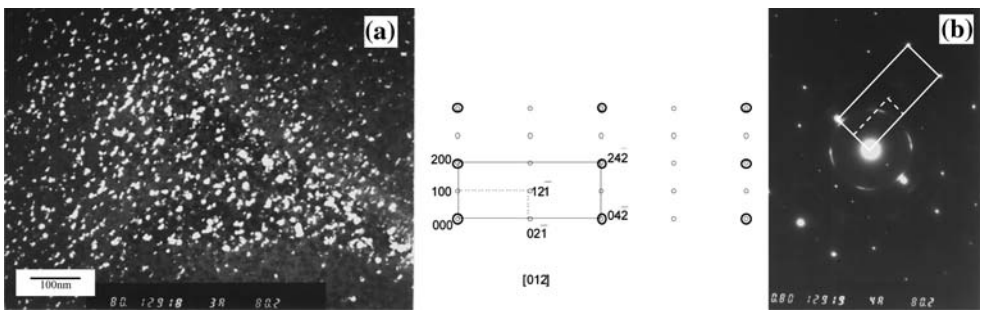

Fig. 7 TEM micrograph and electron diffraction pattern of Ni_3Al in the Ni-based alloy. (**a**) dark-field image, (**b**) electron diffraction pattern

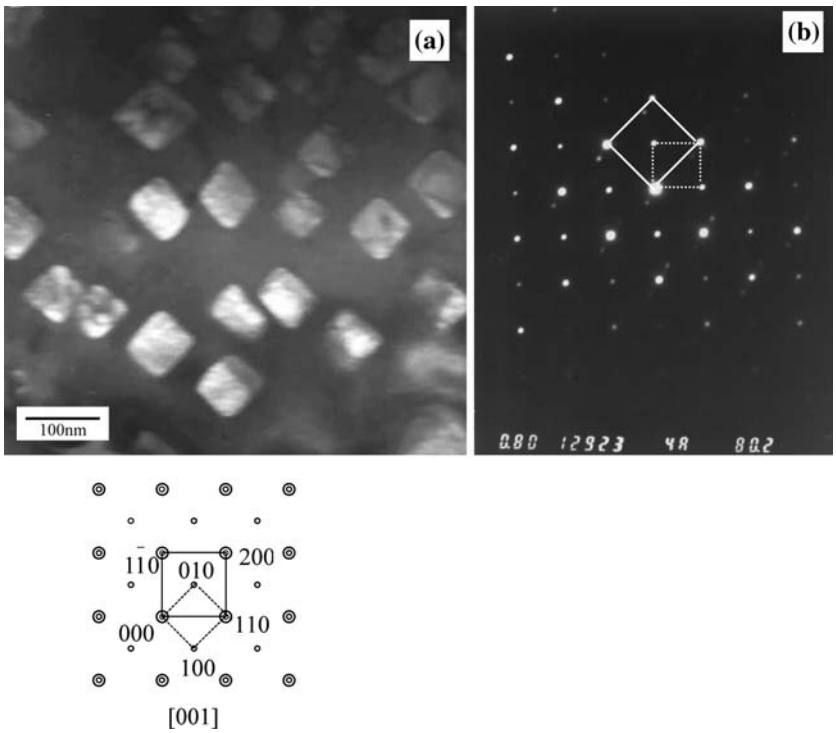

Fig. 8 TEM micrograph and electron diffraction pattern of NiAl in the Ni-based alloy. (**a**) dark-field image, (**b**) electron diffraction pattern

Conclusions

1. The equilibrium thermodynamic analysis indicated that the equilibrium products of the thermite reactions (Fe_2O_3+Cr_2O_3+CrO_3 +NiO+O_2+N_2+TiO_2+C+S+-CaO+Al) contained primarily Al_2O_3, Fe, Ni, Cr, Ni_3Al and NiAl. Depending on the thermite compositions, there could also exist TiC, Cr_7C_3, CrN, CaS and TiN in the equilibrium products.
2. The microstructural investigation showed that the Ni-based alloy prepared by this centrifugal-thermite process consisted of austenite, ferrite, Ni_3Al and NiAl. The existence of Ni_3Al and NiAl in the Ni-based alloy was reconciled with the predictions of the thermodynamic analysis.
3. The thermodynamic analysis showed that as the aluminum content in the starting materials increased, the content of Ni in the products decreased that was replaced by Ni_3Al and NiAl in sequence.
4. As the content of aluminum in the starting materials increased, the adiabatic temperature increased first and then decreased, exhibiting a maximum when the aluminum content reached a certain value. The adiabatic temperature of the thermite reaction system increased linearly with increasing CrO_3 content, which replaced the Cr_2O_3 in the starting materials. Adding CaO to the starting materials reduced the adiabatic temperature.

Acknowledgement This work was financially supported by National Natural Science Foundation of China (NSFC), Grant No.50472100.

References

1. Merzhanov AG (1990) In: Munir ZA, Holt JB (eds) Proceedings of Combustion and Plasma Synthesis of High-temperature Materials. VCH Publishers, New York, pp 1–53
2. Moore JJ, Feng HJ (1995) Prog Mater Sci 39:243
3. Odawara O (1990) J Am Ceram Soc 73:629
4. Munir ZA (1992) Metall Trans A 23:7
5. Yin S (1999) Combustion Synthesis. Metallurgy Industry Publishing House, Beijing
6. Xi W-J (2000) Doctoral Dissertation, University of Science and Technology, Beijing
7. Xi W-J, Yin S, Lai H-Y (2000) J Mater Sci 35:45
8. Xi W-J, Yin S, Lai H-Y (2003) J Mater Proc Tec 137:1
9. White WB, Johnson SM, Dantzig GB (1958) J Chem Phys 28:751
10. Erksson G (1971) Acta Chem Scand 25:2651
11. Kubaschewski O, Alcock CB (1979) Metallurgical thermochemistry. Pergamon Press, UK
12. Knacke O, Kubashewski O, Hesselmann K (1991) Thermochemical properties for inorganic substances. vol 19. Springer-Verlag Heidelberg, Berlin
13. Liang Y-J, Che Y-C (1993) Handbook of thermodynamic data of inorganic materials. Northeast University Press, Shenyang China
14. Sims CT, Hagel WC (1972) The superalloys. A wiley-interscience publication, New York
15. Cline HE, Walter JL (1970) Metall Trans 1:2907
16. JCPDS Cards No. 9–97, 33–0397, 44–1188 and 34–0396